ARTICLE

BIOTECHNOLOGY and BIOENGINEERING

Non-Invasive Self-Referencing Electrochemical Sensors for Quantifying Real-Time Biofilm Analyte Flux

E.S. McLamore,[1,2] D.M. Porterfield,[1,3,4,5] M.K. Banks[2]

[1]Bindley Bioscience Center, Physiological Sensing Facility, Discovery Park, Purdue University, West Lafayette, Indiana; telephone: 806-239-9556; fax: 765-496-3449; e-mail: emclamor@purdue.edu

[2]School of Civil Engineering, Purdue University, West Lafayette, Indiana

[3]Department of Agricultural & Biological Engineering, Purdue University, West Lafayette, Indiana

[4]Department of Horticulture & Landscape Architecture, Purdue University, West Lafayette, Indiana

[5]Weldon School of Biomedical Engineering, Purdue University, West Lafayette, Indiana

Received 18 July 2008; revision received 4 September 2008; accepted 5 September 2008

Published online 19 September 2008 in Wiley InterScience (www.interscience.wiley.com). DOI 10.1002/bit.22128

ABSTRACT: Current techniques for characterizing biofilm physiology lack the signal filtering capability required for quantifying signals associated with real time biologically active transport. Though a great deal was learned from previous investigations, no results have been reported on the characterization of in vivo, real time biofilm flux using non-invasive (non-destructive) techniques. This article introduces the self-referencing technique for applications in biofilm physiology. Self-referencing is a non-invasive sensing modality which is capable of sensing changes in biologically active analyte flux as small as 10 fmol cm^{-2} s^{-1}. Studies directly characterizing flux, as opposed to concentration, have the advantage of quantifying real time changes in biologically active transport which are otherwise lost to background noise. The use of this modality for characterizing biofilm physiology is validated with a reversible enzyme inhibition study. The experiment used self-referencing potentiometric sensors for quantifying real time ammonium and nitrite flux. Amperometric and optical sensing methods, though not presented herein, are also powerful sensing tools which benefit from operation in self-referencing mode. Reversible ammonia monooxygenase inhibition by a copper chelator (thiourea), and subsequent relief by excess copper addition was successfully demonstrated using self-referencing ion-selective microelectrodes for a mature *Nitrosomonas europaea* biofilm.

Biotechnol. Bioeng. 2008;xxx: xxx–xxx.

KEYWORDS: self-referencing; biofilm; flux sensor; physiology; digital differential filtering

Correspondence to: E.S. McLamore

Additional supporting information may be found in the online version of this article.

Introduction

Over the last few decades, there has been an increase in the development of sensors, detectors, and assays for investigating environmental compounds using approaches from the molecular (nanoscale) to the global (macroscale) range. One of the most important applications is in monitoring transport and transformation of compounds in microbial systems (Branda et al., 2005). Recent research has focused on studies investigating biofilm (as opposed to planktonic) microbial phenomena (Parsek and Fuqua, 2003), and a wealth of information was gained from previous biofilm transport studies. However, these studies have been: (1) invasive and/or destructive, (2) based on steady state concentration, (3) had low specificity/selectivity and significant hysteresis, and/or (5) only characterized intrabiofilm or bulk liquid phenomena. In order to sense real time changes in electrochemical character related to biologically active transport, sensors are needed which are capable of non-invasively quantifying analyte flux with detection limits in the sub-micromolar range.

In order to distinguish between sensors, biosensors, detectors, and assays, a clear definition of each is required. Detectors are subject to a high amount of hysteresis (typically via irreversible bonds), and can only quantify compound presence/absence. Assays are defined as the combination of multiple detectors for distinct determination of compound concentration. In contrast to detectors and assays, sensors have little or no hysteresis, and a specific dynamic response time. As opposed to chemical sensors, biosensors have a biological element incorporated in the

recognition or transduction component (Porterfield et al., 2006). Recent reviews of developments in electrochemical sensors (Bakker and Qin, 2006) and sensors, detectors, and assays (Janata and Josowicz, 1998) have been conducted. De Marco et al. (2007) reviewed the use of ISE in complex environmental analysis, and noted the need for techniques which improve sensitivity/selectivity. Reviews have also been conducted for biosensors recently applied for detection of compounds associated with biofilm physiology (Ruzgas et al., 1996).

Though many successful attempts have been made to develop biological and electrochemical sensors/detectors for measuring compound concentration in the biofilm environment (Schramm et al., 2008) to date no literature exists on the use of sensors for measuring biophysical flux. The term biophysical flux denotes that measured extracellular gradients are the direct result of biophysical membrane transport activity, and not passive diffusive gradient flux. Non-invasive and invasive three dimensional biofilm oxygen concentration was quantified using a modified microelectrode (Yu et al., 2004) based on (Revsbech, 1989). Research has been conducted for quantifying ion flux from microbial monolayers (Shabala et al., 2006), though no results have been published for a mature microbial biofilm. Additionally, previous approaches used AC coupled systems, which are subject to capacitor decay. Although studies such as these give insight into fundamental biofilm transport phenomena, electrodes were limited to quantifying concentration values with relatively high detection limits, and were not capable of detecting biophysical flux.

Self-referencing (SR) is a sensing technique which is used for non-invasively measuring real time analyte flux. SR techniques are based on Fick's law of diffusion: $J = -D(\Delta C)(\Delta X^{-1})$ (where J = diffusive analyte flux, D = molecular diffusion constant, C = analyte concentration, and X = diffusionary distance). SR sensors are an extension of the vibrating probe designed for detection of bioelectric current as small as 10 nA/cm^2 (Jaffe and Nuccitelli, 1974). The SR technique "self-corrects" signals produced by ambient drift and noise by oscillating between two locations (termed near pole and far pole) at a fixed excursion distance (Fig. 1) (Kühtreiber and Jaffe, 1990). The method uses a move-wait-measure technique for detecting real time changes in analyte concentration (ΔC) at two points separated by a known excursion distance (ΔX). Use of the SR technique converts static sensors with otherwise low signal-to-noise ratios into dynamic flux sensors capable of filtering out signals not associated with biologically active transport. The SR technique has been validated for potentiometric (Smith et al., 1999), amperometric (Porterfield, 2007), and optical (Porterfield et al., 2006) sensors in the fmol to μmol cm^{-2} s^{-1} range in plant physiology and biomedical applications. Recent progress on SR sensors and their use in measuring flux in biological systems has been reviewed (Porterfield, 2007). This paper introduces the SR technique using potentiometric (ion-selective) microelectrodes, though SR optical and amperometric sensors are also a powerful tool in analyzing biophysical flux in environmental systems.

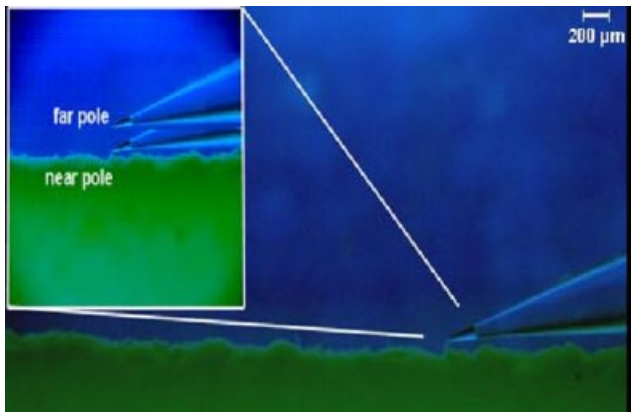

Figure 1. Photograph of self-referencing sensor analysis conducted on a *Nitrosomonas europaea* biofilm immobilized on a hollow fiber silicon membrane (insert depicts near pole and far pole sampling locations). [Color figure can be seen in the online version of this article, available at www.interscience.wiley.com.]

The SR technique is used to demonstrate quantification of analyte flux from an environmental biofilm. The study characterized real time analyte flux during reversible inhibition of a primary enzyme (ammonia monooxygenase) used by the immobilized bacteria. Previous studies have shown reversible inhibition of ammonia monooxygenase for planktonic cells (Vandevivere et al., 1998). Application of SR techniques in the field of biofilm physiology will greatly enhance understanding of many phenomena, including real time external transport and microbial stress response.

Experimental Section

One group of microorganisms that are important in environmental studies are ammonia oxidizing bacteria. The net reaction for oxidation of ammonia by organisms belonging to the *Nitrobacteraceae* family is (Hooper, 1984):

$$NH_3 + O_2 + 2H^+ \rightarrow NH_2OH + H_2O \qquad (1)$$

Equation (1) is catalyzed by membrane bound proteins that include ammonia monooxygenase (AMO) (Bedard and Knowles, 1989) and hydroxylamine oxidoreductase (Suzuki and Kwok, 1974). Subsequent oxidation of hydroxylamine to nitrite is not shown. One of the most commonly studied organisms known to contain AMO is *Nitrosomonas europaea*. AMO inhibition studies are generally grouped by mechanism according to: (1) reversible inhibitors (e.g., thiourea), (2) competitive (active site) inhibitors, or (3) mechanism-based inhibitors (Juliette et al., 1993).

Cell Harvesting and Immobilization

N. europaea were immobilized in upflow membrane-aerated bioreactors (MABR) (McLamore et al., 2007), and transferred to a flowcell for measurement of analyte

flux. Non-porous silicon membranes (Dow Corning Co., Midland, MI) acted as media for microbial attachment, and provided oxygen near the attachment site. McLamore et al. (2007) and others have indicated that MABR limit the formation of anoxic zones near the attachment site for biofilms with a thickness less than 400 μm due to oxygen diffusion from (1) the bulk liquid side, and (2) the attachment (membrane) side. MABRs were constructed from 40 cm long, 10 cm diameter clear PVC attached to 10 cm PVC couplings. Membrane plates were constructed from 2 cm thick clear PVC containing eight 0.64 cm diameter threaded holes, and membranes were fitted through ferrules attached to each membrane plate. Silicon membranes had an outside diameter of 0.17 cm and an inside diameter of 0.08 cm.

Cells were harvested in an environmental growth chamber in the absence of visible light. *N. europaea* and the nutrient medium recipe (ATCC 2265) were obtained from American Type Culture Collection (ATCC, Manassas, VA). ATCC 2265 contained 25.0 mM $(NH_4)_2SO_4$, 43.0 mM KH_2PO_4, 1.5 mM $MgSO_4$, 0.25 mM $CaCl_2$, 10 μM $FeSO_4$, 0.83 μM $CuSO_4$, 3.9 mM NaH_2PO_4, and 3.74 mM Na_2CO_3. Nutrient solution was pumped to the reactors via Cole-Parmer (Vernon Hills, IL) peristaltic pumps and easy load pump heads. An internal recycle line was used to increase convective transport in MABR during immobilization. The influent flowrate, hydraulic retention time, and axial Reynolds (Re_{axial}) number for the MABRs was 5.0 mL/min, 0.8 days, and 250, respectively.

MABR bulk liquid influent and effluent was monitored via in-line grab sampling four times per week to ensure formation of a mature biofilm with steady state growth conditions. The parameters measured (and their respective tolerances for indicating steady state growth) were: change in NH_4^+ or NO_2^- conversion (5%), effluent dissolved oxygen (DO) concentration (>2.0 mg DO/L), and change in effluent pH (±0.5). Bulk liquid influent and effluent samples were analyzed using ion chromatography (IC) (Clesceri et al., 1995) and benchtop meters. IC was conducted using method 4110 (Clesceri et al., 1995) on a Dionex IC (Bannockburn, IL) using an IonPac AS-12A anion for detecting NO_2^- and an IonPac Cs16 cation column for detecting NH_4^+. Bulk DO, pH, and temperature were analyzed using a YSI-85 Meter (Rickly Hydrological Co., Columbus, OH).

A 10.2 cm electrograde Teflon flow cell (McMaster-Carr, Elmhurst, IL) was constructed for measurement of biofilm analyte flux. Measurements were taken within a 7.6 cm long, 5.1 cm wide, and 5.1 cm deep rectangular channel in the middle of the flowcell. New Era (Wantagh, NY) continuous infusion dual syringe pumps were used to supply the liquid-phase solution to the flowcell. The experiments were conducted under static flow conditions to limit background noise due to convective flow. Following transfer to the flowcell, the attached microbes were allowed to stabilize for 30 min, which is within the time period suggested in the literature (Hermanowicz et al., 1995). Biofilms were then exposed to increasing thiourea and $CuCl_2$ concentrations, and real time non-invasive measurements of NH_4^+ flux were taken.

Electrode Fabrication

Ion-selective electrodes (ISE) utilized an immobilized liquid exchange membrane (LIX) and a Ag/AgCl reference electrode, where differences in potential between the near pole and far pole were related to ion activity via the Nernst equation (Piñeros et al., 1998). ISE were constructed using non-filamented, 1.5 mm borosilicate glass capillaries (World Precision Instruments, Inc., Sarasota, FL) pulled on a Sutter P-97 horizontal puller (Flaming-Brown, Sutter instrument Co., Novato, CA). A shank of 3.8–4.0 mm and a tip diameter of approximately 2–5 μm was used throughout. Capillaries were pulled in batches of 50 and placed in stainless steel mesh wire racks, and then silanized using a vapor phase technique from Smith et al. (1999). Pulled, silanized capillaries were stored in a desiccating chamber and had a lifetime of 2–3 weeks.

Immediately prior to use, microelectrodes were backfilled with electrolyte and then front filled with ammonium LIX (cocktail A), or nitrite LIX (Schaller et al., 1994) (Fluka, St. Louis, MO). The electrolyte used for NH_4^+-selective electrodes was 10 mM NH_4Cl, and the electrolyte used for NO_2^- selective electrodes was 10 mM $NaNO_2$ + 10 mM NaCl. For front filling electrodes, a 100 μm tip diameter silanized pipette was dipped into stock LIX to produce a cocktail column approximately 1 mm in length. This pipette and the electrode were placed into a dual micromanipulator mounted under a binocular microscope and adjusted to the same focal plane. The tip of the microelectrode was placed inside the tip of the LIX pipette. If necessary, slight pressure was applied to the electrode to adjust column length via a pressure control system. A LIX column length of 200 μm was used for NH_4^+-selective electrodes, and a column length of 300 μm was used for NO_2^- selective electrodes. The filled electrodes were then inserted into a half-cell microelectrode holder (World Precision Instruments, Inc., Sarasota, FL) fitted with an electrolitically plated Ag/AgCl wire; detailed methods for chloriding silver wires may be found in Smith et al. (1999). The return pathway (reference probe) for the circuit was 3 M KCl immobilized in 3% agar injected into 1.5 mm polyethylene tubing inserted in a microelectrode holder half cell (World Precision Instruments, Inc., Sarasota, FL).

Self-Referencing Hardware

SR hardware included a vibration isolation table with Faraday cage (Technical Manufacturing Co., Peabody, MA), camera/zoomscope and sensor(s) mounted on a head stage controlled by a motion control system (MCS) (Fig. 2). Automated Scanning Electrode Technique (ASET) software was used for data acquisition (A/D) and control functions

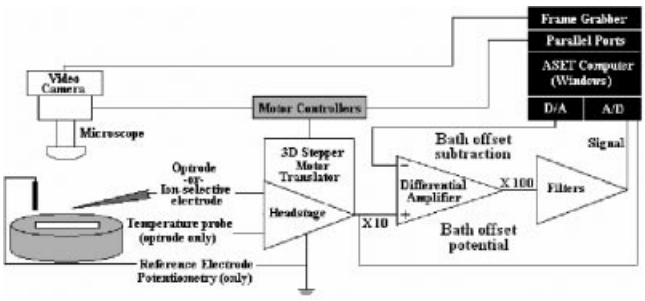

Figure 2. Schematic of self-referencing system.

(D/A) (Science Wares, Falmouth, MA). ASET can support multiple SR sensors simultaneously in one, two, or three dimensional analysis of analyte flux (Faszewski and Kunkel, 2001; Donini and O'Donnell, 2004). Care should be taken when conducting multi-dimensional analyses, as these studies can require sophisticated data processing techniques. The A/D board with DC-coupled differential amplifier, low/high pass filters, and video/data acquisition system were obtained through Applicable Electronics, Inc. (Sandwich, MA).

The move-wait-measure technique employed by ASET utilized a bath offset function for periodic cancellation of background current at the origin (near pole) position. The ASET bath offset is a variable input autozero function which utilizes a hardware gateway for a D/A channel output from the PC to provide background cancellation. DC coupled systems have the advantage of a specific bath offset, and are not subject to capacitor decay (as in AC coupled systems). The sample rate for all experiments was 1,000 V readings per second. Where applicable, error bars and $\pm$ indicate one standard deviation (unbiased) of the arithmetic mean of voltage readings. Though the IPA-2 amplifier filters out signals exceeding 10 KHz, noise is unavoidable due to the high input resistance of the microelectrodes. The peak-to-peak signal noise for a 1 GΩ resistor is approximately 2.5 μV (data averaged over 10 s).

Use of an oscillation frequency (0.2–0.5 Hz) and excursion distance (20–60 μm) within the range suggested in the literature (Kühtreiber and Jaffe, 1990) ensures that background noise and drift will be common between the two point, and mechanical motion of the electrode will not significantly disrupt the concentration gradient. The oscillation frequency for NH_4^+ electrodes (0.30 Hz) was similar to the 0.32 Hz suggested by Donini and O'Donnell (2004) with a few exceptions. All wait times and measure times used by Donini and O'Donnell (2004) were 1.0 and 2.0 s, respectively. Wait and measure protocol for SR NH_4^+ electrodes was: 0.20 s bath wait time, 0.15 s bath measurement time, 0.30 s wait time at origin, 0.80 s measurement at origin, 0.65 s wait at sample position, and 0.85 s measurement time at sample position. The oscillation frequency used for NO_2^- detection was 0.42 Hz with the following settings: 0.20 s bath wait time, 0.20 s bath measurement time, no wait time at origin, 0.60 s measurement at origin, 0.20 s. wait at sample position, and 0.80 s. measurement time at sample position. The excursion distance for NH_4^+ and NO_2^- selective microelectrodes were 30 and 40 μm, respectively.

Static Electrode Calibration

ISE behavior is quantified via accordance to the Nernst (or Nikolsky-Eisenmann) equation. The Nikolsky-Eisenmann equation for any ISE in standard conditions is an extension of the Nernst equation and accounts for the effect of interfering ions (Eq. 2) (Diamond, 1998). A complete list of interfering compounds for ion-selective electrodes may be found in Umezawa et al. (1995). Characterization of ISE response time should be conducted following the guidelines developed by the international union of pure and applied chemistry (IUPAC) (Maccà, 2004).

$$E = E^o + s \times \ln(C_i + \Sigma K_{\text{pot}} C_{\text{k}}^{z_k/z_i}) \qquad (2)$$

where, E is the electrode potential (mV), E^o the electrode half cell constant (mV), s the Nernst slope ($59.16/z_i$), z_i the valence of primary ion, z_k the valence of interfering ion, C_i the concentration of primary ion (mM), C_k the concentration of interfering ion (mM), and K_{pot} the potentiometric selectivity coefficient.

Nernstian electrode calibration was conducted before and after each experiment by adding NH_4Cl or $NaNO_2$ to ATCC 2265 medium in the 0.5–500 mM range. Electrodes with Nernstian slopes outside the $(59.16/z_i) \pm 2$ mV/decade change in concentration were discarded per IUPAC recommendations (Bakker and Qin, 2006). Selectivity was tested by altering electrode cell assembly based on results reported in Donini and O'Donnell (2004). K_{pot} values were determined for the interfering ions contained in ATCC 2265 nutrient medium (or byproducts of their biodegradation) based on the recipe reported by Bakker et al. (2000). For NH_4^+-selective electrodes, the ions tested (and their concentrations) were: K^+ (0.1–200 mM), Na^+ (0.01–1.0 mM), Ca^{2+} (0.1–10 mM), and Mg^{2+} (0.1–10 mM). For NO_2^- selective electrodes, the ions tested (and their concentrations) were: HPO_4^{2-}(1–100 mM), HCO_3^-(0.1–100 mM), and Cl^-(0.1–10 mM).

Dynamic Electrode Calibration

After combining with the Fick equation, the equation defining ion-specific flux for a SR ion-selective (SRIS) electrode becomes Equation (3). Use of the SR technique in this manner produces positive values for efflux, and negative values for influx. When operating ISE in SR mode for quantifying diffusive flux, E^o and K_{pot} cancel from Equation

(2), and electrode potential is only a function of primary ion activity and Nernst slope. In cases where significant transport of interfering ion(s) occurs, investigators must alter Equation (3) by including the K_{pot} term from Equation (2). Alternatively, one may simultaneously measure ion flux of primary and interfering ions with multiple SRIS electrodes.

$$J = -D\left[\frac{\Delta C_i - \Delta C_{ref}}{\Delta X}\right] = -D\left[\frac{(10^{E_1 - b/s} - 10^{E_2 - b/s}) - \Delta C_{ref}}{\Delta X}\right] \quad (3)$$

where, J is the Ion-specific flux ($\mu mol\,cm^{-2}\,s^{-1}$), E_1 the electrode potential at near pole (mV), E_2 the electrode potential at far pole (mV), b the y-intercept of Nernst plot (mV), ΔC_{ref} the difference in potential at reference location (mV), and ΔX the excursion distance between near/far pole (μm).

The ΔC_{ref} in Equation (3) was calculated by ASET software in the same manner as ΔC_i, and was taken at a point 5 mm from the diffusional source/sink. The inclusion of ΔC_{ref} is a post measurement filter technique subtracted from all flux values to correct for background noise caused by mechanical motion of the sensor in the bath solution, and is typically in the 1–100 $fmol\,cm^{-2}\,s^{-1}$ range (Kühtreiber and Jaffe, 1990).

Dynamic calibration of microelectrodes was conducted using step back experiments (SBE) in abiotic conditions similar to those expected during biological experiments. SBE are necessary for increasing accuracy and minimizing solution mixing by electrode movement. SBE were conducted by moving the sensors through analyte gradients in a step-wise manner. Initial step sizes were 1–2 μm, but increased as the change in flux asymptotically approached zero. Following accurate determination of the concentration gradient, the electrode was returned to each location, and SR flux measurements recorded with a fixed excursion distance. For maximum accuracy the excursion distance used in SR mode was in the same direction as the linear profile obtained in static (non-oscillating) mode. An additional benefit of conducting SBE is direct quantification of the mass boundary layer thickness (δ) formed at the solid–liquid interface. The value of δ is typically taken as the distance from the solid–liquid interface where $\Delta C/\Delta X \approx 0$ (Welty et al., 2001).

Alginate beads containing target ions were used as an artificial source. Alginate beads were fabricated by mixing 6.0 mL of sterile ion solution and 31 mL of sterile sodium alginate solution. This solution was then dripped into a Petri dish filled with crosslinking solution (0.1 M-strontium chloride) using a 1 mL pipette (Heitzer et al., 1994) to produce beads with a diameter of approximately 3 mm. Alginate beads were kept in crosslinking solution for 2 h at 5°C, and stored in ion solution at room temperature prior to use. Beads were allowed to stabilize in bath solutions for 30 min prior to SBE. The bath solution consisted of primary ion solution at 10% of the artificial source concentration (e.g., 10 mM NH_4Cl) and a salt solution (e.g., 90 mM $MgCl_2$) with the total molarity being equal to that of the artificial source (e.g., 100 mM NH_4Cl).

When characterizing signals in the sub mV range, temporal drift and random system noise can produce misleading data (e.g., positive drift would lead to a negative differential artifact). For systems with temporal drift artifacts, an additional signal processing technique is required. The digital differential filtering (DDF) technique removes signals associated with random system noise and temporal drift while leaving the spatial differentials intact. The traditional method of calculating ΔC is to subtract the far pole concentration ($C_{1,n}$) from the near pole concentration ($C_{0,n}$) for each measurement cycle (n). The DDF algorithm filters signals every half cycle using Equation (4), where $C_{0,n+1}$ is the near pole concentration for measurement cycle $n+1$.

$$dC = \frac{(C_{0,n} - C_{1,n}) + (C_{0,n+1} - C_{1,n})}{2} \quad (4)$$

Results from SBE analysis were compared to theoretical diffusion models based on static concentration, and the correlation coefficient between the predicted and actual data was reported as the dynamic efficiency (ε). The one-dimensional predictive model was developed assuming isotropic diffusion from a sphere 3 mm in diameter based on empirical values of mass boundary layer thickness. Dynamic efficiency is used to optimize SR experimental protocol (Kunkel et al., 2006). The value of ε is a function of sensor response time, selectivity, specificity, and oscillation frequency (see Appendix for characterization of electrode response time, selectivity, and specificity). Optimizing this value is critical since signals associated with background noise decrease with the square root of measurement time, and SR sensors with low ε values lose their noise filtering capability. Though researchers have attempted to use ε as a correction factor for flux data, this approach was avoided, and efficiency was maximized by altering sensor electrochemical/physical configuration. Dynamic efficiency optimization was conducted by altering oscillation frequency within the 0.2–0.5 Hz range suggested by Jaffe and Nuccitelli (1974).

Ion flux was measured at six locations 1–2 μm from the biofilm surface. After recording the flux at position six, four 10 μL additions of 1.0 M-thiourea (Acros Organics, West Chester, PA) were added and real time in vivo measurements of NH_4^+ surface flux were taken. Flux was recorded for a period of 10 min during each interval dose addition. Following the final addition of thiourea, steady state NH_4^+ flux was again recorded at each of the six locations. The sensor was then returned to location six, and eight 20 μL additions of 10 mM $CuCl_2$ were added to the system. Flux was again recorded for a period of 10 min during each

interval dose addition. Following the final dose of $CuCl_2$, steady state flux was recorded at each location. All analyses were additionally filtered using a two cycle algorithm presented in Equation (4).

Results and Discussion

Morphologically homogenous, mature biofilms were grown on silicon membranes in MABR. Biofilm thickness and surface roughness was relatively homogenous based on visual observation and still imaging. Effluent MABR data indicated steady state concentrations existed; effluent NO_2^- and NH_4^+ conversion were $62 \pm 2\%$, and $57 \pm 4\%$, respectively, effluent pH was 6.77 ± 0.63, and effluent DO was 2.3 ± 0.2 mg O_2/L.

Sensor Calibration

Static calibration of electrodes was conducted before and after all experiments, and electrodes failing to meet Nernstian criteria ($59.16/z_i$ mV per decade change in primary ion concentration) were discarded. Electrode cell assembly was validated by calibration in the presence of interfering ions. The Hoffmeister series and their respective values for NH_4^+-selective microelectrodes were: K^+ $(0.93 \pm 0.09) > Mg^{2+}(3.60 \pm 0.05) > Na^{2+}(3.42 \pm 0.08) > Ca^{2+}(4.22 \pm 0.01)$. Standard deviation (unbiased) of the arithmetic mean was calculated for six experiments. The logarithmic NH_4^+ selectivity coefficient for K^+ (0.93) was lower than values (2.04) reported in the literature (Ghauri and Thomas, 1994). This discrepancy is primarily due to the high K^+/NH_4^+ ratio (1.73) in the ATCC 2265 medium. The Hoffmeister series and their respective values for NO_2^- selective microelectrodes were: HPO_4^{2-} $(2.10 \pm 0.06) > Cl^-$ $(3.02 \pm 0.04) > HCO_3^-$ (3.02 ± 0.09), which are similar to values reported in the literature (Schaller et al., 1994). The selectivity coefficients are slightly different due to the relatively high concentration of phosphate and chloride in the ATCC 2265 nutrient medium. Details on selectivity analysis may be found in the Appendix. When utilizing ISE in the SR modality, it is not necessary to measure interfering ion activity unless significant biological flux of the interfering ion occurs within the gradient; recall that the K_{pot} term on the right side of Equation (2) cancels during calculation of ΔC.

Abiotic SBE using SR NH_4^+ and NO_2^- selective electrodes were conducted for 10, 100, and 500 mM alginate beads to demonstrate the range of flux values which may be characterized using the SR technique. Additionally, SBE were conducted using SR NH_4^+ and NO_2^- selective electrodes on a *N. europaea* biofilm immobilized on a silicon membrane. Reference flux measurements (ΔC_{ref}) for each experiment were taken 5 mm from the liquid–solid interface. Error bars indicate one standard deviation (unbiased) of the arithmetic mean of voltage readings ($n = 6 \times 10^5$).

For SBE on abiotic alginate beads, dynamic efficiency values of SR NH_4^+-selective electrodes were above 0.92 in the 10–500 mM range (Fig. 3). This range of flux values (fmol to pmol $cm^{-2} s^{-1}$) is relevant for most biological systems, including microbial biofilms. The concentration gradient for each experiment may be calculated using Fick's Law and values of the molecular diffusion coefficient and excursion distance given in the experimental section. For example, near the surface of the 500, 100, and 10 mM alginate beads, the concentration gradient was approximately 75 μM NH_4^+, 1.6 μM NH_4^+, and 9.8 nM NH_4^+, respectively. The thickness of the mass boundary layer for

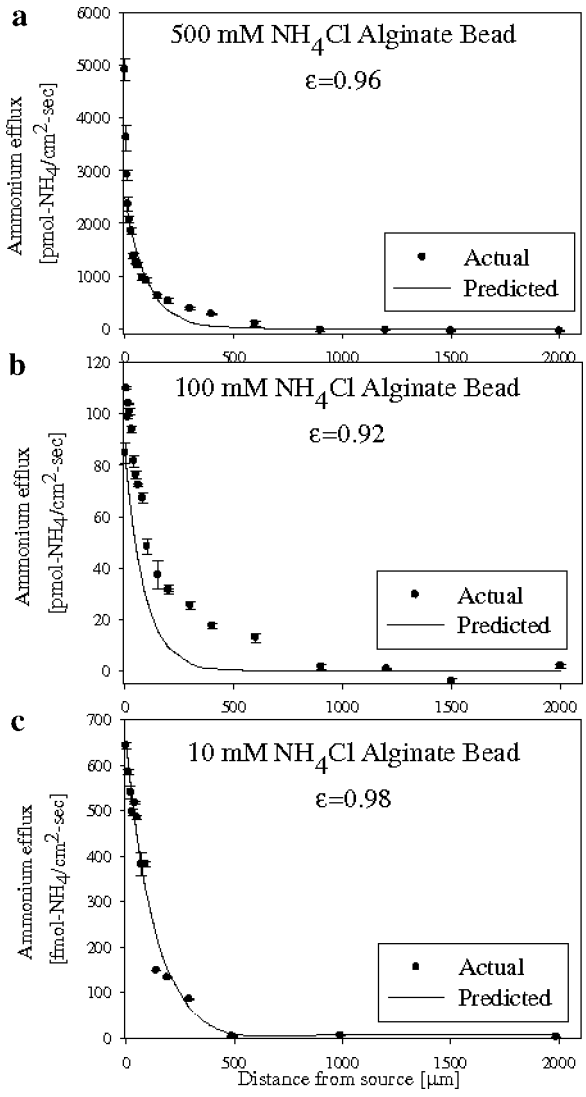

Figure 3. SR NH_4^+-selective electrode step back experiment on abiotic alginate bead with concentrations of: **(a)** 500 mM NH_4Cl, **(b)** 100 mM NH_4Cl, and **(c)** 10 mM NH_4Cl.

500, 100, and 10 mM NH_4Cl alginate beads was approximately 900, 780, and 495 μm, respectively. The mass boundary layer thickness for 500, 100, and 10 mM $NaNO_2$ alginate beads was approximately 500, 440, and 360 μm, respectively (SBE data not shown). These values were significantly lower than the values obtained for NH_4Cl alginate beads, which is reflected in the value of the molecular diffusion coefficient; 20×10^{-5} $cm^2\,s^{-1}$ for NH_4Cl and 7.6×10^{-5} $cm^2\,s^{-1}$ for $NaNO_2$ (Horvath, 1985). There are many sources for the discrepancy in the predicted and actual data in SBE. The factors which were investigated (and subsequently ruled out) were electrolyte backfill type/concentration, electrode tip diameter/shape, and LIX column length. Current studies are aimed at optimizing ionophore cocktail mixture for characterizing biofilm physiology.

NH_3 is the substrate for AMO, based on significant reductions in AMO activity with increasing pH (McCarty, 1999). Measurement of NH_4^+ flux (as opposed to NH_3) was validated using a pH microelectrode; the pH at the surface of the biofilm (6.71) was significantly lower than the pK_a of NH_4^+ (9.2). SBE conducted on a *N. europaea* biofilm indicated a maximum NH_4^+ influx of 591 pmol $cm^{-2}\,s^{-1}$, and a maximum NO_2^- efflux of 643 pmol $cm^{-2}\,s^{-1}$ (Fig. 4). The mass boundary layer thickness for NH_4^+ influx was approximately 470 μm, which was less than the value for the NO_2^- SBE (585 μm). This discrepancy was due to the difference in the diffusion coefficient, and is not due to biologically active transport. The mass boundary layer thickness for nitrite was significantly less than the value approximated from data published by DeBeer et al. (1997) using static (concentration) NO_2^--selective electrodes. Although previous studies using traditional microelectrode sensing techniques were able to characterize analyte concentration in the mass boundary layer, they were not capable of quantifying real time (non-steady state) changes in analyte flux. Values reported using SRIS electrodes demonstrate the temporal variability not captured using traditional techniques.

The real time response of a *N. europaea* biofilm to increasing copper chelation by thiourea and subsequent relief by addition of $CuCl_2$ demonstrate the real time sensing capability of the SR technique. A bare membrane in a bath solution of autoclaved ATCC 2265 was used as a zero control to ensure abiotic chemical activity did not affect microelectrode behavior (data not shown). Reversible AMO inhibition was noted at all of the sampling locations except position two (Fig. 5a). Data from position two was included to demonstrate the spatial heterogeneity in bioactivity which has been reported in previous studies. AMO inhibition by copper chelation occurred at concentrations as low as 1.5 mM-thiourea, and concentrations above 6 mM-thiourea had no additional effect (Fig. 5b and c). Concentrations below 60 μM had no significant effect in a 24 h study (data not shown). Voltage differences at position one during steady state, post thiourea dosing, and post copper dosing were approximately 25, 0.1, and 22 μV, respectively. 140 μM $CuCl_2$ was required to re-establish basal steady state ammonium influx levels, which is similar to values reported for mixed culture nitrifying biofilms in a municipal wastewater treatment plant; significant increases in ammonia oxidation were noted for bulk liquid copper concentrations as low as 100 μM (Ensign et al., 1993). The significant signal variation during copper addition was not due to electrical/mechanical noise. Multiple repetitions ($n = 9$) of this experiment indicated that the use of copper as a cofactor in multiple cellular processes (other than AMO activity) is the cause of the relatively high variation in flux during the last section of the experiment. Other possible causes of signal variation could be due to local copper toxicity. To ensure that copper cytoxicity did not occur, a potassium selective SRIS electrode was used to measure pre and post-copper

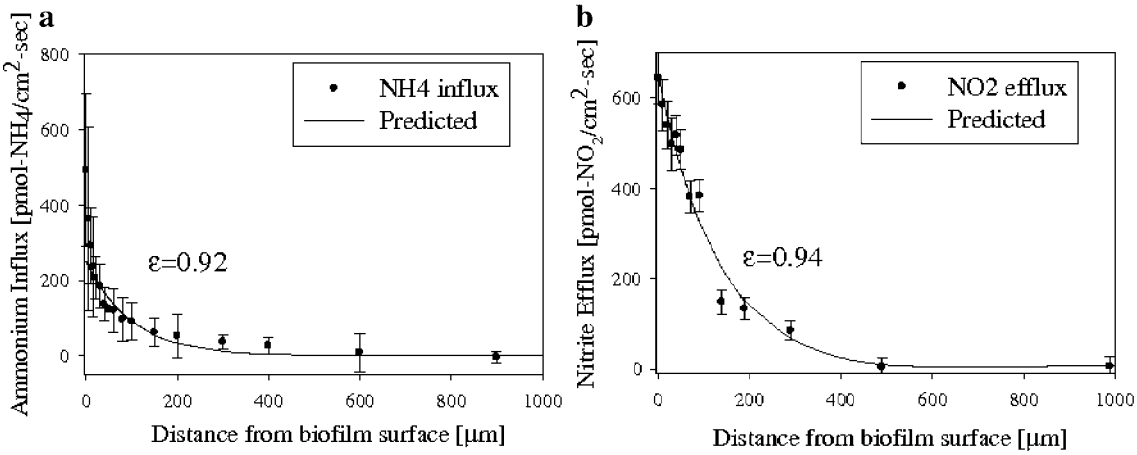

Figure 4. Step back experiments on a *Nitrosomonas europaea* biofilm immobilized on a silicon membrane for (**a**) SR NH_4^+-selective microelectrode and (**b**) SR NO_2^- selective electrode.

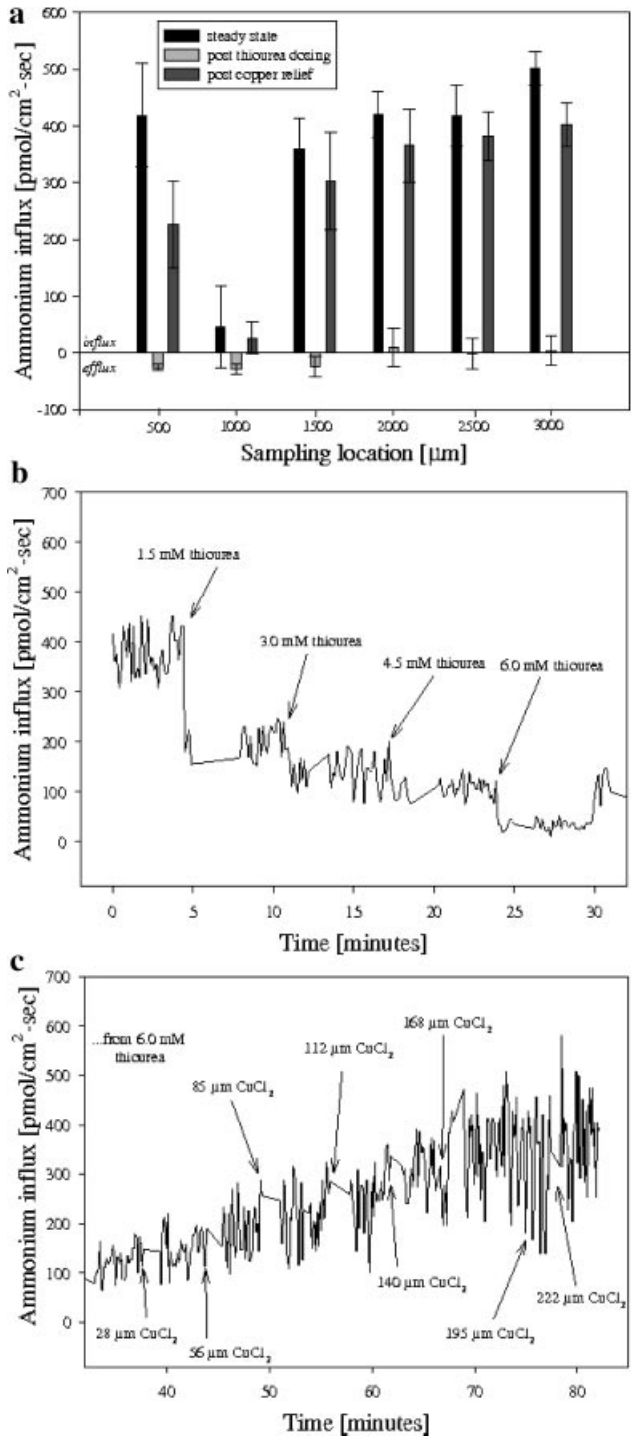

Figure 5. Ammonium influx from a *Nitrosomonas europaea* biofilm. **a**: Steady state ammonium surface influx at six sampling locations, (**b**) real time ammonium influx with increasing thiourea concentration, and (**c**) real time ammonium influx with increasing copper chloride concentration.

exposure potassium flux. There was no significant difference in potassium efflux before (0.15 ± 0.08 fmol cm^{-2} sec^{-1}) or after (0.16 ± 0.10 fmol cm^{-2} sec^{-1}) relief of thiourea chelation by excess copper addition. The SR modality has the unique capability of quantifying real time non-steady state changes in biofilm analyte flux. The changes in analyte concentration (ca. 1–100 nM NH_4^+) reported are below the detection limit of current traditional ISE. Studies aimed at characterizing and/or modeling fundamental biofilm physiology and/or microbial stress response mechanisms will benefit from the use of such techniques.

Conclusions

Characterization of in vivo mass transport phenomena in biological systems requires sensing techniques capable of non-invasively quantifying real time species flux. The self-referencing modality is a noise filtering technique with real time temporal resolution and detection limits as low as 10 fmol cm^{-2} s^{-1}. Self-referencing ion-selective microelectrodes were used to quantify real time biofilm analyte flux. A reversible enzyme inhibition study was used to demonstrate the types of in vivo responses which may be characterized using the self-referencing modality. The results presented herein clearly demonstrate the benefits of utilizing SR sensors for characterizing real time biologically active transport in biofilms. Future studies conducted on pure and mixed culture ammonia-oxidizing bacteria will simultaneously measure NH_4^+, NO_2^-, pH, K^+, Ca^{+2}, and O_2 biophysical flux. Results from these studies will aid in modeling of biofilm systems, and allow characterization of real time biological response to chemical toxin/stressor exposure.

The authors would like to thank Alan Shipley (Applicable Electronics, Inc.) for his technical support and John Shaff for his help with electrode fabrication techniques. This work was funded with support from the School of Civil Engineering at Purdue University.

References

Bakker E, Qin Y. 2006. Electrochemical sensors. Anal Chem 78:3965–3983.

Bakker E, Pretsch E, Buhlmann P. 2000. Selectivity of potentiometric ion sensors. Anal Chem 72(6):1127–1133.

Bedard C, Knowles R. 1989. Physiology, biochemistry, and specific inhibitors of CH_4, NH_4^+, and CO oxidation by methanotrophs and nitrifiers. Microbiol Rev 53(1):68–84.

Branda S, Vik A, Friedman L, Kolter R. 2005. Biofilms: The matrix revisited. Trends Microbiol 13(1):20–26.

Clesceri LS, Greensburg AE, Eaton AD. 1995. Standard methods for the examination of water and wastewater, 20th edition. Washington, DC: American Public Health Association.

de Marco R, Clarke G, Pejcic B. 2007. Ion-selective electrode potentiometry in environmental analysis. Electroanalysis 19(19–20):1987–2001.

DeBeer D, Schramm A, Santegoeds CM, Kuhl M. 1997. A nitrite microsensor for profiling environmental biofilms. Appl Environ Microbiol 63(3):973–977.

Diamond D. 1998. Principles of chemical and biological sensors. New York: John Wiley & Sons, Inc.

Donini A, O'Donnell MJ. 2004. Analysis of Na^+, Cl^-, K^+, H^+ and NH_4^+ concentration gradients adjacent to the surface of anal papillae of the mosquito Aedes aegypti: Application of self-referencing ion-selective microelectrodes. J Exp Biol 208:603–610.

Ensign SA, Hyman MR, Arp DJ. 1993. In vitro activation of ammonia monooxygenase from *Nitrosomonas europaea* by copper. J Bacteriol 175:1971–1980.

Faszewski E, Kunkel JG. 2001. Covariance of ion flux measurements allows new interpretation of *Xenopus laevis* oocyte physiology. J Exp Zool 290:652–661.

Ghauri MS, Thomas JDR. 1994. Evaluation of an ammonium ionophore for use in poly(vinyl chloride) membrane ion-selective electrodes: Solvent mediator effects. Analyst 119(11):2323–2326.

Heitzer A, Malachowsky K, Thornnard JE, Bienkowski JR, White DC, Sayler GS. 1994. Optical biosensor for environmental on-lone monitoring of naphthalene and salicylate bioavailability with an immobilized bioluminescent catabolic reporter bacterium. Appl Environ Microbiol 60(5):1487–1494.

Hermanowicz SW, Schindler U, Wilderer P. 1995. Fractal structure of biofilms: New tools for investigation of morphology. Water Sci Technol 32(8):99–105.

Hooper AB. 1984. Ammonia oxidation and energy transduction in the nitrifying bacteria. In: Strohl WR, Tuovinen OH, editors. Microbial chemoautotrophy. Columbus: Ohio State University Press. pp. 133–167.

Horvath AL. 1985. Handbook of aqueous electrolyte solutions: Physical properties, estimation and correlation methods. New York: John Wiley & Sons, Inc.

Jaffe L, Nuccitelli R. 1974. An ultrasensitive vibrating probe for measuring steady extracellular currents. J Cell Biol 63:614–628.

Janata J, Josowicz M. 1998. Chemical sensors. Anal Chem 70:179R–208R.

Juliette LY, Hyman MR, Arp DJ. 1993. Inhibition of ammonia oxidation in nitrosomonas europaea by sulfur compounds: Thioethers are oxidized to sulfoxides by ammonia monooxygenase. Appl Environ Microbiol 59(11):3718–3727.

Kühtreiber WM, Jaffe LF. 1990. Detection of extracellular calcium gradients with a calcium-specific vibrating electrode. J Cell Biol 110:1565–1573.

Kunkel JG, Cordeiro S, Xu Y, Shipley AM, Feijó JA. 2006. Use of non-invasive ion-selective microelectrode techniques for the study of plant development. In: Volkov AG, editor. Plant electrophysiology: Theory and methods. Berlin: Springer. pp. 109–137.

Maccà C. 2004. Response time of ion-selective electrodes: Current usage versus IUPAC recommendations. Anal Chim Acta 512:183–190.

McCarty GW. 1999. Modes of action of nitrification inhibitors. Biol Fertil Soils 29:1–9.

McLamore E, Jackson WA, Morse A. 2007. Abiotic transport in a membrane-aerated bioreactor. J Membr Sci 298:110–116.

Parsek MR, Fuqua C. 2003. Biofilms 2003: Emerging themes and challenges in studies of surface-associated microbial life. J Bacteriol 186(14):4427–4440.

Piñeros MA, Shaff JE, Kochian LV. 1998. Development, characterization and application of a cadmium-selective microelectrode for the measurement of cadmium fluxes in roots of Thlaspi species and wheat. Plant Physiol 116:1393–1401.

Porterfield DM. 2007. Measuring metabolism and biophysical flux in the tissue, cellular and sub-cellular domains: Recent developments in self-referencing amperometry for physiological sensing. Biosens Bioelectron 22:1186–1196.

Porterfield DM, Rickus JL, Kopelman R. 2006. Non-Invasive Approaches to Measuring Respiratory Patterns Using a PtTFPP Based, Phase-Lifetime, Self-Referencing Oxygen Optrode. Proceedings of SPIE, Vol. 6380.

Revsbech NP. 1989. An oxygen microsensor with a guard cathode. Limnol Oceanogr 32(2):474–478.

Ruzgas T, Csoregi W, Emneus J, Gorton L, Marko Varga G. 1996. Peroxidase-modified electrodes: Fundamentals and application. Anal Chem Acta 330(2–3):123–138.

Schaller U, Bakker E, Spichiger UE, Pretsch E. 1994. Ionic additives for ion-selective electrodes based on electrically charged carriers. Anal Chem 66(3):391–398.

Schramm A, DeBeer D, Gieseke A, Amann R. 2000. Microenvironments and distribution of nitrifying bacteria in a membrane-bound biofilm. Appl Environ Microbiol 2(6):680–686.

Shabala L, Ross S, McMeekin T, Shabala S. 2006. Non-invasive microelectrode ion flux measurements to study adaptive responses of microorganisms to the environment. FEMS Microbiol Rev 30:472–486.

Smith PJS, Hammar K, Porterfield DM, Sanger RH, Trimarchi JR. 1999. Self-referencing, non-invasive, ion selective electrode for single cell detection of trans-plasma membrane calcium flux. Microsc Res Tech 46:398–417.

Suzuki I, Kwok SC. 1974. Ammonia or ammonium ion as substrate of oxidation of *Nitrosomonas europaea* cells and exracts. J Bacteriol 120: 556–558.

Umezawa Y, Umezawa K, Sato H. 1995. Selectivity coefficients for ion-selective electrodes: Recommended methods for reporting $K_{pot(A,B)}$ values. Pure Appl Chem 67(3):507–518.

Vandevivere P, Ficara E, Terras C, Julies E, Verstraete W. 1998. Copper-mediated selective removal of nitrification inhibitiors from industrial wastewaters. Environ Sci Technol 32:1000–1006.

Welty J, Wicks CE, Wilson RE, Rorrer GL. 2001. Fundamentals of momentum, mass, and heat transfer, 4th edition. New York: John Wiley & Sons, Inc.

Yu T, de la Rosa C, Lu R. 2004. Microsensor measurement of oxygen concentration in biofilms: from one dimension to three dimensions. Water Sci Technol 49(11–12):353–358.